RESEARCH ARTICLE

Effect of Trichostatin A on CNE2 Nasopharyngeal Carcinoma Cells - Genome-wide DNA Methylation Alteration

Xiao-Li Yang[1], Cheng-Dong Zhang[1], Hua-Yu Wu[1], Yong-Hu Wu[1], Yue-Ning Zhang[1], Meng-Bin Qin[1], Hua Wu[1], Xiao-Chun Liu[3], Xing Lina, Shao-Ming Lu [1,2]*

Abstract

Trichostatin A (TSA) is a histone deacetylase (HDAC) inhibitor. We here investigated its effects on proliferation and apoptosis of the CNE2 carcinoma cell line, and attempted to establish genome-wide DNA methylation alteration due to differentially histone acetylation status. After cells were treated by TSA, the inhibitory rate of cell proliferation was examined with a CCK8 kit, and cell apoptosis was determined by flow cytometry. Compared to control, TSA inhibited CNE2 cell growth and induced apoptosis. Furthermore, TSA was found to induce genome-wide methylation alteration as assessed by genome-wide methylation array. Overall DNA methylation level of cells treated with TSA was higher than in controls. Function and pathway analysis revealed that many genes with methylation alteration were involved in key biological roles, such as apoptosis and cell proliferation. Three genes (DAP3, HSPB1 and CLDN) were independently confirmed by quantitative real-time PCR. Finally, we conclude that TSA inhibits CNE2 cell growth and induces apoptosis *in vitro* involving genome-wide DNA methylation alteration, so that it has promising application prospects in treatment of NPC *in vivo*. Although many unreported hypermethylated/hypomethylated genes should be further analyzed and validated, the pointers to new biomarkers and therapeutic strategies in the treatment of NPC should be stressed.

Keywords: Trichostatin A - nasopharyngeal carcinoma - CNE2 – methylation - acetylation

Asian Pac J Cancer Prev, **15 (11)**, 4663-4670

Introduction

Nasopharyngeal carcinoma (NPC) is a rare malignant tumor in most parts of the world, but much more endemic in Southern China and Southeast Asia (Wee et al., 2010). The incidence of nasopharyngeal carcinoma is highest in those regions where the annual incidence is as high as 80 per 100, 000 individuals (Spano et al., 2003). Currently, radiotherapy remains the mainstay of therapy for NPC, but the therapeutic effect is not always satisfactory (Qin et al., 2008). For patients with advanced disease, concomitant chemotherapy shows better therapeutic efficacy than radiotherapy given alone (Chan et al., 2005; Jamshed et al., 2014). Even with combined treatment, approximately 30% of patients experience treatment failure within 5 years, and treatment outcomes vary widely (Lee et al., 2010; Liu et al., 2013). It is urgent to find out more efficient therapeutic strategies and new biomarkers.

Tumors are characterized by aberrant transcriptional silencing of genes via epigenetic mechanisms, such as DNA methylation and post-translational modifications of the histones (Eriksson et al., 2013). DNA Methylation occurs mainly in the context of cytosines followed by guanines (CpGs) (Laurent et al., 2010). The methylation process is controlled by a family of DNA methyltransferases (DNMTs) that catalyze the transfer of methyl groups from S-adenosyl-L-methionine to the 5' position of cytosine bases in the CpG dinucleotide (Fabbri et al., 2007). Altered DNA methylation, such as global hypomethylation or regional hypermethylation, is one of the most consistent epigenetic changes in human cancer (Gao et al., 2013). As for histones, transcriptional repression is in general associated with low levels of histone acetylation, whereas transcriptionally active genes are associated with highly acetylated core histones (Johnstone and Licht, 2003). Acetylation is believed to separate the basic N-termini of histones from DNA that then becomes more accessible to transcription factors (Cecconi et al., 2003). Thus, histone acetylation leads to gene activation, while histone deacetylation leads to a tighter histone-DNA interaction and, accordingly, to gene repression (Cecconi et al., 2003). Histone acetylation status is regulated by the opposing actions of histone acetyl-transferases (HATs) and histone deacetylases (HDACs) (Smith and Denu, 2009). During the last years HDAC-inhibitors have become one of the most promising classes of chemotherapeutics with profound antitumour effects (Glaser, 2007), and are successfully used to inhibit cell growth of lots of

*[1]Medical Scientific Research Center, Guangxi Medical University, Nanning, [2]Center for Reproductive Medicine, Provincial Hospital Affiliated to Shandong University, Jinan, [3]Department of laboratories, The People's Hospital of Guangxi Zhuang Autonomous Region, Nanning, China *For correspondence: Shaoming_lu@163.com*

carcinoma cells in vitro (McBain et al., 1997; Shin et al., 2000).

Trichostatin A (TSA) was originally characterized as an anti-fungal antibiotic and later identified as specific HDAC-inhibitor (Tsuji et al., 1976). TSA belongs to the category of the hydroxamic acid HDAC inhibitors and is one of the most potent HDAC inhibitors that has been an invaluable tool in vitro experiments (Zhang et al., 2012) to probe and elucidate mechanisms related to apoptosis (PA Marks and VM Richon, 2001). TSA has been reported to modulate transcriptional activity, thereby affecting a broad variety of cellular processes, such as cell cycling, differentiation, apoptosis, and culminating in the inhibition of cell proliferation, angiogenesis, and metastasis (Zhang, 2008). Selker et al. (1998) have demonstrated that the TSA could cause selective loss of DNA methylation in Neurospora. Zhang et al. provides strong in vitro evidence that TSA inhibits cancer growth by triggering an apoptotic pathway, which is via a caspase-dependent manner. Subsequently, a series of studies indicate that increase of histone acetylation by TSA was associated with a significant decrease in global methylation (Ou et al., 2007). However, genome-wide demethylation induced by TSA does not affect all methylated tumor suppressor genes equally suggesting that induction of acetylation and demethylation by TSA shows some gene selectivity (Ou et al., 2007).

Studies using TSA on various cancer cell lines such as glioma cells, bladder cancer cells, and leukemic cells have demonstrated inhibition of cellular proliferation, induction of cell cycle arrest, and subsequent induction of apoptosis (Platta et al., 2007). However, the effect of TSA on NPC cells has been rarely examined. In the present study, we explore the effect of TSA on proliferation and apoptosis of NPC CNE2 cells, and attempted to reveal the alteration of DNA methylation caused by changed histone acetylation status using genome-wide methylation array after TSA administrated. .

Materials and Methods

Materials

Human Nasopharyngeal carcinoma cell line CNE2 was purchased from Shanghai Institute of Biochemistry and Cell Biology (SIBCB, Shanghai, China). Trichostatin A (TSA) was purchased from Cell Signaling Technology, Inc. (Danvers, MA, USA.).RPMI1640, trypsin, penicillin-streptomycin and fetal bovine serum (FBS) were purchased from Life Technologies Corp (Carlsbad, CA, U.S.A.). All other chemicals were of the highest grade commercially available.

Cell culture

Nasopharyngeal carcinoma CNE2 cell line was purchased from the Institute of Cell Biology, Chinese Academy of Sciences. The cells were cultured in RPMI1640 medium supplemented with 10 % FBS, 100 U/ml penicillin, and 100 μg/ml streptomycin at 37 °C in a humidified incubator with 5 % CO_2.

Cell proliferation assay

CNE2 cells proliferation was measured by Cell Counting Kit-8 detection kit (Beyotime, China). Cells were seeded into a 96-well plate at 5×10^3 cells per well with RPMI 1640 containing 10% FBS, and allowed to adhere for 24h. After the medium was removed, cells were washed with PBS, replace the previous medium with serum-free medium. Various concentrations of TSA (0, 100, 200, 300, 400, 500, 600 nM) were added to each well, respectively. At 6, 12, 24 and 36 h after incubation, CCK-8 solution was applied at 10 μl per well and followed by 2-h incubation at 37 °C. Absorbance values of all wells were then determined at 450 nm in Microplate Reader (Bio-Rad, USA). All experiments were conducted in triplicate.

FCM analysis

Annexin-V/propidium iodide (PI) double staining assay was performed by using the Annexin V-FITC apoptosis detection kit (Sigma-aldrich, USA) as described by the manufacture's instruction. Briefly, 1×10^6 cells per well with various treatments described for 24h were harvested and washed with cold PBS in 24-well plates. The cells were washed with PBS twice and resuspended in 1× Binding buffer, followed by incubated with Annexin V-FITC conjugate and PI for 15 min to protect from light at room temperature. Cells were analyzed by flow cytometry (FCM) analysis using BD CELLQuest software (BD Biosciences, USA).

DNA extraction and sodium bisulfite conversion

DNA extraction was performed on CNE2 cells treated with 0nm and 400nm TSA for 24h using the QIAamp DNA Mini Kit (Germantown, MD, USA). Bisulfite conversion of genomic DNA was done with the EZ DNA methylation Kit (Zymo Research, D5002) by following manufacturer's protocol.

Microarray

Bisulfite-converted genomic DNA was analyzed using Illumina's Infinium Human Methylation27 Beadchip Kit (Illumina Inc., USA). Beadchip contains 27,578 CpG loci covering more than 14,000 human RefSeq genes at single-nucleotide resolution. Chip process were performed by using reagents provided in the kit and following manufacturer's manual. Data were extracted and summarized using genomeStudio software. Arrays that did not pass quality control in terms of b-distributions and expected *p*-values across the arrays were removed. Methylation scores represented as β values were generated for each site using Illumina Genome Studio Methylation module v1.8 (Illumina Inc., USA) and were computed based on the ratio of methylated to methylated plus unmethylated signal outputs.

Data-dependent bioinformatics for network analysis

Functional classification of identified proteins was accomplished by using Entrez Gene (http://www.ncbi.nlm.nih.gov/entrez/query.fcgi?db_gene) and DAVID (http:/www.david.abcc.ncifcrf.gov). Proteins with multiple functions were assigned to those that are best known. Pathway module analysis of the functional clusters was performed by KEGG.

Table 1. Sequences of the Primers for RT-QPCR

Name	Strand	Sequence (5'–3')
HSPB1	Forward	AAGGATGGCGTGGTGGAGA
	Reverse	AGGGGACAGGGAGGAGGAAA
DAP3	Forward	GGGTATTGTACCGCTGAGGG
	Reverse	CTTGGCCGGGTCATTCTCAT
CLDN	Forward	GGGAGACGACAAAGTGAAGAAG
	Reverse	CTGCCCAGCCAATAAAGATG
NDFIP1	Forward	CTCCACCTTACAGCAGCATTTC
	Reverse	AGTAGCTTCAGCCTTGGTCCTC
GRK5	Forward	AGAGACTCTTCAAGCGGCAG
	Reverse	GGTTCTACGTCGACGGGATG
β-actin	Forward	TGAGGCACTCTTCCAGCCT
	Reverse	CCGATCCACACGGAGTACTTG

RT-QPCR analysis

The mRNAs were isolated from CNE2 cells using Trizol reagent from Invitrogen. Up to 1 μg of RNA was reversed-transcribed using the PrimeScript RT reagent Kit with gDNA Eraser (Takara, Japan). cDNA was amplified in SYBR green master mix (Roche, Germany) with the Realplex (Eppendorf, Germany). Conditions used for amplification were as follows: an initial 5 minute 95°C period followed by 40 cycles of 95°C for 15 seconds, 60°C for 1 min. Relative mRNA levels were determined using the $2^{-\Delta\Delta Ct}$ interpretation and normalized to the β-actin. The primer pairs for each gene were designed with Primer Premier 5.0 software; Sequences of all the primers are shown in Table 1.

Statistical analysis

All experiments were performed independently three times, the results a were shown as mean values ± standard deviation (SD), and statistical analyses were performed using SPSS17.0 software. The statistical differences were calculated using a standard one-way ANOVA and two-tailed unpaired Student's t test. $P < 0.05$ was considered as statistically significant. In all graphs, *, # indicates significant difference.

Results

The cell proliferation inhibition effects of TSA

The cell proliferation inhibition effects of TSA in CNE2 cells were detected by CCK8 assay. The CNE2 cells were treated with 0, 100, 200, 300, 400, 500, 600nM TSA respectively for 24, 48 and 72 h respectively. As shown in Figure 1, the TSA inhibited the proliferation of CNE2 cells was reduced in a time- and dose-dependent manner. From 300 nM to 500 nM, the inhibitory rate increased quickly. Some changes of apoptosis could be seen by light microscopy, such as cytoplasmic vacuoles and apoptotic bodies (Figure 1B). About 48h, most of the cells were dead (Data not shown).

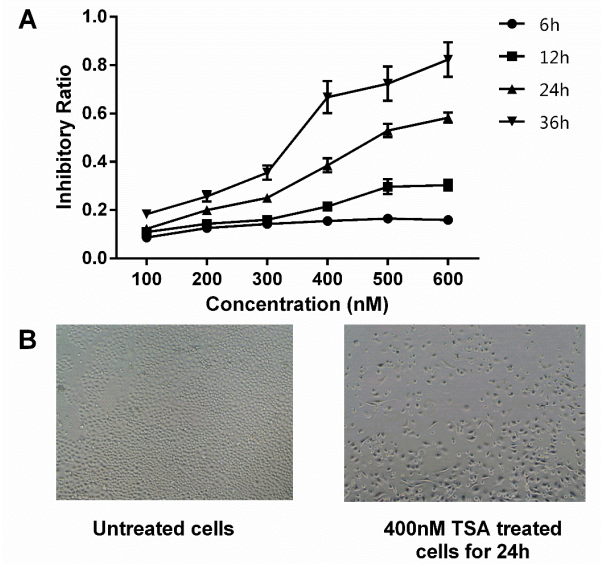

Figure 1. Effects of TSA on Cell Proliferation. A.CNE2 cells were treated with different concentrations of TSA for 6, 12, 24 and 36 h. Cell inhibitory rate was measured with CCK8 assay. B. Cellular morphology (100×). CNE2 cells were treated with 0 nM and 400nM for 24h

The cell cycle arrest and apoptosis induced by TSA

Annexin V-FITC/PI double staining and FCM analysis were performed to evaluate the ability of TSA. As Figure 2 shows, the apoptosis of cells treated with TSA for 24h significantly increased compared with that of untreated cells ($p<0.05$).The inhibitory rate was highest in the cells treated with 400 nM TSA than that in other groups.

Global Methylation Profile

Global DNA methylation profiles were measured using Illumina Infinium Human Methylation27 BeadChips, which target 14, 475, total refseq genes, 12, 833 well-annotated genes described in the NCBI CCDS database, 144 methylation hotspots in cancer genes, 982 cancer-related targets and 110 miRNA promoters. We performed genome-wide methylation profiling between cells treated with TSA for 24h and control cells (0 nm, 24h). Preliminary analysis was conducted after background correction, then sites on the sex chromosomes were removed from the analysis on the array. 26468 CpG sites obtained. The average methylation intense of cells treated with 400nM TSA was lower than that of matched control (Figure 3A and Figure 3B), but they had the familiar frequency distribution (Figure 3B). Furthermore, most of the sites had positive correlation between TSA

Table 2. Characteristics of Genes Selected to Verify

Symbol	Name	Gene ID	Strand	TSS	CPG Island	CPG Island Locations	Methylation
HSPB1	heat shock 27kD protein 1	3315	Forward	9	TRUE	7:75769511-75771539	UP
CLDN7	Clostridium perfringens enterotoxin receptor-like 2	1366	Reverse	120	TRUE	17:7104851-7107119	UP
DAP3	Death Associated Protein 3	7818	Forward	1422	TRUE	1:153924032-153926450	UP
NDFIP1	Nedd4 Family Interacting Protein 1	80762	Forward	287	TRUE	5:141468002-141469424	DOWN
GRK5	G protein-coupled receptor kinase 5	2869	Forward	354	TRUE	10:120955944-120958030	DOWN

TSS, Distance to transcription start site; Up, Hypermethylation; Down, Hypomethylation; All methylation locis are before TSS

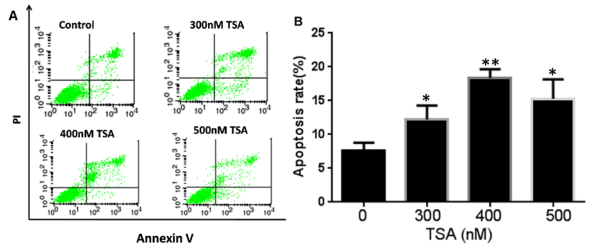

Figure 2. Cell Apoptosis was Detected by Annexin V-FITC/PI Double Staining and FCM Analysis. Cells were Treated with 0, 300, 400 and 500 nM TSA for 24h. A. Apoptosis rates were measured by FCM analysis after AnnexinV/PI staining. The upper right quadrant (An+/PI+) is counted as apoptotic cells. B. Percentage of dual-positive (Annexin V and PI were positive) cells from three independent experiments was quantified and presented as mean ± SD. *p<0.05 compared with untreated cells, ** p<0.05 compared with untreated cells

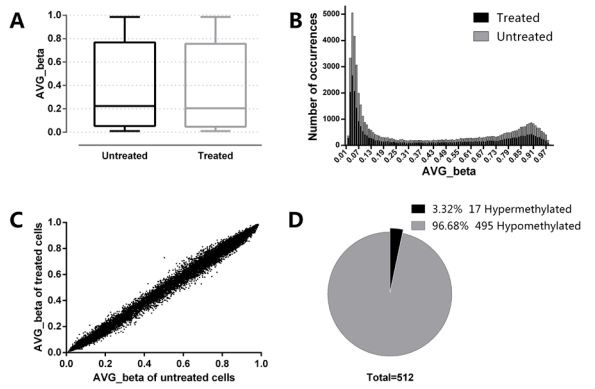

Figure 3. Average Methylation Level of CNE2 Cells were Measured by Array. Cells were treated with 0nM and 400nM TSA for 24h. Methylation scores were represented as beta values. AVG_beta: average beta. A. The illustrative box plots represented the mean, 25th percentile, 75th percentile and range of all the 26,468 CpG sites. B. Frequency distribution of average beta of all the 26, 468 CpG sites. C. Scatter plots of average beta of of all the 26, 468 CpG sites. D. Pie chart representing the proportions of 1.5 fold-change of hypomethylated and hypermethylated sites

treated cells and untreated cells, just a few not (Figure 3C). The comparison of methylation between groups was based on the difference in mean beta value (Avgβ) of each CpG site. Empirically, we selected the sites that the ratio between the Avgβ of cells treated with 400nM TSA and Avgβ of control cells is >1.5 or <0.67 as a threshold and *P*-value less than 0.05. There were 512 CpG sites that significantly differed in methylation level between the cells treated with TSA for 24h and control cells (0nm, 24h). Among all significant CpG sites, 97% were significantly hypomethylated (covering 488 genes) and 3% were significantly hypermethylated (covering 17 genes) in the cells treated with TSA, compared to control (Figure 3D).

Functional categories of the identified hypermethylated and hypomethylated gene associated with TSA

By searching Entrez Gene (http://www.ncbi.nlm.nih.gov/entrez/query.fcgi?db_gene) and DAVID (http://www.david.abcc.ncifcrf.gov), we found most of the

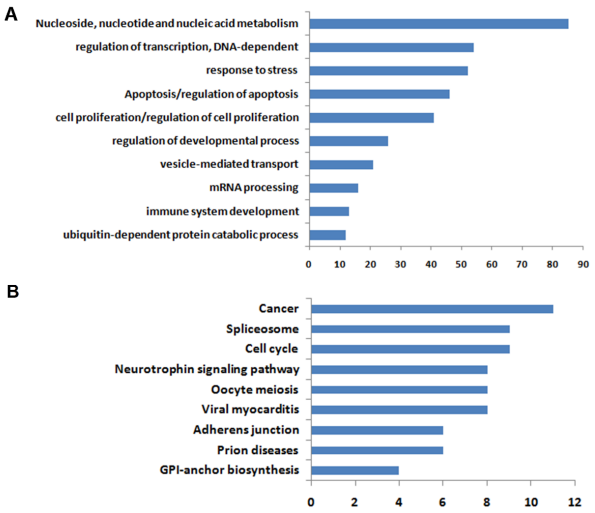

Figure 4. Functional Categories and Pathway Modules of Genes which Methylation Level were Changed. A. The distribution of genes which methylation changed in different functional Categories. The identified genes were analyzed by bioinformatics tools using Entrez Gene and DAVID. B. Pathway modules

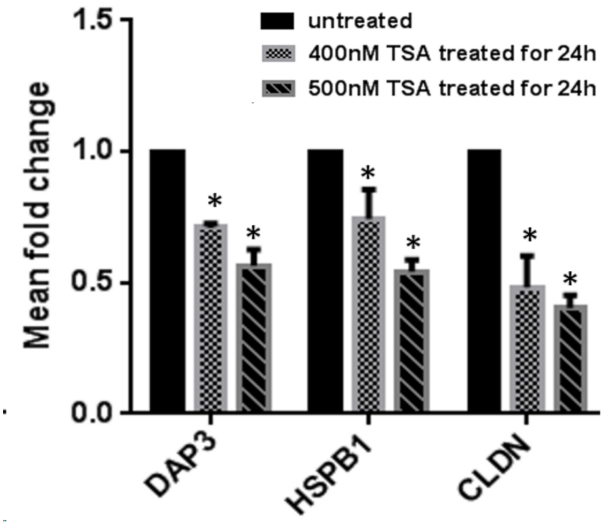

Figure 5. qPCR Validation of Methylation Array Data. Test genes are listed on the x axis, and the mean fold change in expression in each sample group (400nM or 500nM), compared with that in the reference group (untreated), is shown on the y axis. Fold changes were calculated using the ddCT method, in which fold change data are represented as 2–ddCT. Error bars depict the standard error of the mean dCT values. Significant differences (P<0.05) are denoted with an asterisk

hypermethylated and hypomethylated gene associated with TSA treatment identified by methylation array were clustered in some functional categories. As shown in Figure 4A, these functional categories include nucleoside/nucleotide and nucleic acid metabolism, regulation of transcription (DNA-dependent), response to stress, apoptosis/regulation of apoptosis, cell proliferation/regulation of cell proliferation, regulation of developmental process, vesicle-mediated transport, mRNA processing, immune system development and ubiquitin-dependent protein catabolic process. Furthermore, after pathway module analysis by KEGG, just a 69 genes were defined to 9 known pathway module: cancer, cell cycle, spliceosome,

neurotrophin signaling pathway, adherens junction, etc. Since drugs inducing apoptosis remain the main chemotherapeutic agents in medical oncology, we focus on the genes associated with apoptosis and cell proliferation. At the meanwhile, many genes did not report that their metylation alteration was related to NPC tumorigenesis.

The change of gene Expression after TSA treatment

The mRNA expression of DAP3, HSPB1, CLDN, NDFIP1 and GRK5 was detected by RT-qPCR (Table 2). mRNA expression of NDFIP1and GRK5 did not change significantly. DAP3, HSPB1 and CLDN exhibited a significant decrease in the cells treated by TSA (400nM and 500nM for 24h compared with the control cells (Figure 5).

Discussion

Recent studies revealed that TSA, a HDAC inhibitor, has significant antitumor activity in many types of cancer cells. Expression levels of many genes are altered by TSA due to global suppression of histone deacetylation. In the present study, effects of TSA on NPC were investigated. Furthermore, genome-wide DNA methylation alteration regulated by TSA also been involved.

Accumulation of genetic and epigenetic alterations results in the development of NPC. As a main epigenetic change, histone hyperacetylation is generally associated with chromatin decondensation, which increases the accessibility of DNA to binding proteins as well as transcriptional activity, whereas histone hypoacetylation contributes to chromatin condensation and transcriptional repression (Tse et al., 1998; Wang et al., 2001). The interplay between HDACs and HATs differentially and reversibly regulates the acetylation status of the N-terminal region of histones as well as non-histone proteins (Johnstone and Licht, 2003; Marks et al., 2004; Dokmanovic et al., 2007). Transcriptional activators recruit HATs and are associated with acetylated chromatin (Gregory et al., 2001; Eberharter and Becker, 2002). In contrast, transcriptional repressors and co-repressors interact with HDACs and their binding to promoters correlates with loss of histone acetylation (Villar-Garea and Esteller, 2004; Saha and Pahan, 2006). Thus, HDACs function in opposition to HATs by removal of charge neutralizing acetyl groups from the histone lysine tails thereby inducing transcriptional repression through chromatin condensation (Roth et al., 2001; Thiagalingam et al., 2003). Aberrant HDAC expression and activity has been observed in numerous malignancies. These provided the basis for the development of HDAC inhibitors as anticancer therapies. It is possible to interfere with lysine acetylation by a pharmacological approach using HDAC-inhibitor. The final outcome of HDAC-inhibitor treatment is broad and cell type dependent (Shiva and Willems, 2014).

In our experiment, we found that TSA could induce CNE2 cells to death (Figure 1A), and this cell death included apoptotic cell death (Figure 2). At present, drugs inducing apoptosis remain the main chemotherapeutic agents in medical oncology (Lefranc and Kiss, 2006). Although cisplatin-based chemotherapy has shown promising effects with NPC, acquired resistance to chemotherapy has been one of the most important clinical problems (Kartalou and Essigmann, 2001; Siddik, 2003). Therefore, it is still an urgent need to explore new therapeutic strategies.

DNA methylation is another important epigenetic mechanism of regulating gene expression. In general, promoter DNA methylation is correlated with gene repression. When a gene is hypermethylated, especially in its promoter region, transcription is usually diminished (Vaillant and Paszkowski, 2007). Duan X et al. reported that Aberrant hypermethylation of HOXA2 led to low RNA expression in NPC tumors and cells (Li et al., 2013). Tian F, et al. found five hypermethylated genes (RASSF1, CDKN2A, DLEC1, DAPK1 and UCHL1) using methylation-specific PCR, and got a conclusion that Screening DNA hypermethylation of tumor suppressor genes in serum was a promising approach for the diagnosis of NPC (Tian et al., 2013). Du C, et al. posed Arsenic trioxide could reverse LMP1-mediated methylation and silencing of E-cadherin gene in NPC, and restore the gene's promoter activity and expression, and indicate a potential therapeutic strategy for NPC (Du C et al., 2012).

Oncogenes could be silenced by inducing methylation of their promoter regions. Some researchers have postulated that reversal of both promoter methylation and histone deacetylation may lead to a greater degree of gene transcription than the reversal of one mechanism alone (Gilbert et al., 2004). An importance of epigenetic aberrations, including promoter hypermethylation and histone modifications, has been indicated for the processes of carcinogenesis and pathogenesis of Cholangiocarcinoma (Limpaiboon, 2012). Furthermore, it has been found DNA methylation and histone modification regulate silencing of OPG during NPC progression (Lu et al., 2009). Although TSA is being evaluated in preclinical cancer models and in clinical trials, little is known about its mechanism of action. Since both DNA methylation and histone modifications are strongly implicated in the process of gene transcriptional activity, their relationship is a heated point (Ma et al., 2011). However, there is no consensus on which epigenetic mechanism initiates and steers this communication (Ma et al., 2011). Some experiments supported that DNA methylation guide histone modifications (Irvine et al., 2002; Locke and Martienssen, 2006; Huettel et al., 2007; Wozniak et al., 2007), however, other studies show contradictory evidence. Some researches demonstrated that increase in histone acetylation by Trichostatin A (TSA) was associated with a significant decrease in global methylation (Ou et al., 2007; Arzenani et al., 2011). In this study, we used a genome-wide DNA methylation microarray to measured global DNA methylation levels at 26468 CpG sites after TSA treatment. Overall DNA methylation levels of cells treated by TSA is lower than that in control. Furthermore, among 26468 CpG sites, we found 512 CpG sites to significantly differ in methylation level; 97% (512 loci) of which were hypomethylated (1.5 folder change).

Function and pathway analysis showed that most of genes of methylation alteration were clustered in diverse

functional categories. As shown in Figure 4, TSA could affect many genes which had different functions, such as nucleic acid metabolism, transcription, immune, apoptosis, proliferation and ubiquitin. It indicated that TSA has diverse functions as other studies reported (Harrison and Dexter, 2013; Sigalotti et al., 2013). We focus on the genes associated with vital biological function, and did not report that their metylation alteration was related to NPC tumorigenesis before. Thus, some genes associated with apoptosis, proliferation and cell cycle were validated by RT-qPCR. We speculated that those genes may be involved in the PNC tumorigenesis.

HSPB1 coded protein is induced by environmental stress and developmental changes. It is involved in stress resistance and actin organization and translocates from the cytoplasm to the nucleus upon stress induction. In our experiments, this gene was hypermethylated, and mRNA expression was lower after TSA treatment. High level of HSPB1 expression in cancer cells promotes tumourigenesis, metastasis and anti-cancer drug resistance (Gibert et al., 2013). Wang JJ, et al. found up-regulated HSPB1 may play many important roles in the pathogenesis of colorectal cancer (Wang et al., 2012). HSPB1 also drives epithelial mesenchymal transition, metastasis, and circulating tumor cells in prostate cancer (Selker, 1998). It was identified as a radioresistance-related protein in NPC cells (Zhang et al., 2012). HSPB1 was thought as a new cancer therapeutic target (Arrigo and Gibert, 2012). DAP3 (death associated protein 3) is a GTP-binding constituent of the small subunit of the mitochondrial ribosome, and is responsible for regulating apoptosis induced by various stimuli (Harada et al., 2010). It is overexpressed in human thyroid oncocytictumours, and may participate in mitochondrial maintenance and play a role in the balance between mitochondrial homoeostasis and tumourigenesis (Jacques et al., 2009). CLDN (claudin 7) encodes a member of the claudin family. Claudins are integral membrane proteins and components of tight junction strands. Tight junction strands serve as a physical barrier to prevent solutes and water from passing freely through the paracellular space between epithelial or endothelial cell sheets, and also play critical roles in maintaining cell polarity and signal transductions (Lu et al., 2013). Claudin-7 is frequently overexpressed in ovarian cancer and promotes invasion (Dahiya et al., 2011). Increased expression of CLDN contributes to an anti-apoptotic role in TNF-alpha-induced apoptosis (Liu et al., 2012). Upregulated CLDN expression confers resistance to cell death ofnasopharyngeal carcinoma cells (Lee et al., 2010). Claudin 4 and claudin 7 may be a novel biomarker for the prediction of distant metastasis and unfavorable prognosis in NPC (Hsueh et al., 2010).

The mechanism that TSA effect the NPC cells are still quite complex, and the details and pathways involved should be clarified in the future. In conclusion, we first used genome-wide methylation arrays to identify genes methylated in CNE2 cells treated by TSA. Our study demonstrates that DNA methylation is involved in proliferation inhibitor and apoptosis induce by TSA. Although many novel methylated genes should be further analyzed and validated, it may still provide some new biomarkers and therapeutic strategies in the treatment of NPC.

Acknowledgements

The authors gratefully acknowledge the financial support provided by the Foundation for the Guangxi Key Laboratory for Prevention & Treatment of Regional High-Incidence Diseases (N0. KFJJ2010-35). We would like to thank Editage for providing editorial assistance.

References

Arrigo AP, Gibert B (2012). HspB1 dynamic phospho-oligomeric structure dependent interactome as cancer therapeutic target. *Curr Mol Med*, **12**, 1151-63.

Arzenani MK, Zade AE, Ming Y, et al (2011). Genomic DNA hypomethylation by histone deacetylase inhibition implicates DNMT1 nuclear dynamics. *Mol Cell Biol*, **31**, 4119-28.

Cecconi D, Scarpa A, Donadelli M, et al (2003). Proteomic profiling of pancreatic ductal carcinoma cell lines treated with trichostatin-A. *Electrophoresis*, **24**, 1871-8.

Chan AT, Leung SF, Ngan RK, et al (2005). Overall survival after concurrent cisplatin-radiotherapy compared with radiotherapy alone in locoregionally advanced nasopharyngeal carcinoma. *J Natl Cancer Inst*, **97**, 536-9.

Dahiya N, Becker KG, Wood WH 3rd, et al (2011). Claudin-7 is frequently overexpressed in ovarian cancer and promotes invasion. *PLoS One*, **6**, e22119.

Dokmanovic M, Clarke C, Marks PA (2007). Histone deacetylase inhibitors: overview and perspectives. *Mol Cancer Res*, **5**, 981-9.

Du C, Yang P, Zhang G, et al (2012). Effect of Arsenic trioxide on EBV LMP1 mediated E-cadherin silencing in nasopharyngeal carcinoma. *Head Neck Oncol*, **4**, 55.

Eberharter A, Becker PB (2002). Histone acetylation: a switch between repressive and permissive chromatin. Second in review series on chromatin dynamics. *EMBO Rep*, **3**, 224-9.

Eriksson I, Joosten M, Roberg K, Ollinger K (2013). The histone deacetylase inhibitor trichostatin A reduces lysosomal pH and enhances cisplatin-induced apoptosis. *Exp Cell Res*, **319**, 12-20.

Fabbri M, Garzon R, Cimmino A, et al (2007). MicroRNA-29 family reverts aberrant methylation in lung cancer by targeting DNA methyltransferases 3A and 3B. *Proc Natl Acad Sci USA*, **104**, 15805-10.

Gao J, Wang L, Xu J, et al (2013). Aberrant DNA methyltransferase expression in pancreatic ductal adenocarcinoma development and progression. *J Exp Clin Cancer Res*, **32**, 86.

Gibert B, Simon S, Dimitrova V, et al (2013). Peptide aptamers: tools to negatively or positively modulate HSPB1 (27) function. *Philos Trans R Soc Lond B Biol Sci*, **368**, 20120075.

Gilbert J, Gore SD, Herman JG, Carducci MA (2004). The clinical application of targeting cancer through histone acetylation and hypomethylation. *Clin Cancer Res*, **10**, 4589-96.

Glaser KB (2007). HDAC inhibitors: clinical update and mechanism-based potential. *Biochem Pharmacol*, **74**, 659-71.

Gregory PD, Wagner K, Horz W (2001). Histone acetylation and chromatin remodeling. *Exp Cell Res*, **265**, 195-202.

Harada T, Iwai A, Miyazaki T (2010). Identification of DELE, a novel DAP3-binding protein which is crucial for death receptor-mediated apoptosis induction. *Apoptosis*, **15**, 1247-55.

Harrison IF, Dexter DT (2013). Epigenetic targeting of histone deacetylase: therapeutic potential in Parkinson's disease. *Pharmacol Ther*, **140**, 34-52.
Hsueh C, Chang YS, Tseng NM, et al (2010). Expression pattern and prognostic significance of claudins 1, 4, and 7 in nasopharyngeal carcinoma. *Hum Pathol*, **41**, 944-50.
Huettel B, Kanno T, Daxinger L, et al (2007). RNA-directed DNA methylation mediated by DRD1 and Pol IVb: a versatile pathway for transcriptional gene silencing in plants. *Biochim Biophys Acta*, **1769**, 358-74.
Irvine RA, Lin IG, Hsieh CL (2002). DNA methylation has a local effect on transcription and histone acetylation. *Mol Cell Biol*, **22**, 6689-96.
Jacques C, Fontaine JF, Franc B, et al (2009). Death-associated protein 3 is overexpressed in human thyroid oncocytic tumours. *Br J Cancer*, **101**, 132-8.
Jamshed A, Hussain R, Iqbal H (2014). Gemcitabine and cisplatin followed by chemo-radiation for advanced nasopharyngeal carcinoma. *Asian Pac J Cancer Prev*, **15**, 899-904.
Johnstone RW, Licht JD (2003). Histone deacetylase inhibitors in cancer therapy: is transcription the primary target. *Cancer Cell*, **4**, 13-8.
Kartalou M, Essigmann JM (2001). Mechanisms of resistance to cisplatin. *Mutat Res*, **478**, 23-43.
Laurent L, Wong E, Li G, et al (2010). Dynamic changes in the human methylome during differentiation. *Genome Res*, **20**, 320-31.
Lee AW, Tung SY, Chua DT, et al (2010). Randomized trial of radiotherapy plus concurrent-adjuvant chemotherapy vs radiotherapy alone for regionally advanced nasopharyngeal carcinoma. *J Natl Cancer Inst*, **102**, 1188-98.
Lee JW, Hsiao WT, Chen HY, et al (2010). Upregulated claudin-1 expression confers resistance to cell death of nasopharyngeal carcinoma cells. *Int J Cancer*, **126**, 1353-66.
Lefranc F, Kiss R (2006). Autophagy, the Trojan horse to combat glioblastomas. *Neurosurg Focus*, **20**, E7.
Li HP, Peng CC, Chung IC, et al (2013). Aberrantly hypermethylated Homeobox A2 derepresses metalloproteinase-9 through TBP and promotes invasion in Nasopharyngeal carcinoma. *Oncotarget*, **4**, 2154-65.
Limpaiboon T (2012). Epigenetic aberrations in cholangiocarcinoma: potential biomarkers and promising target for novel therapeutic strategies. *Asian Pac J Cancer Prev*, **13**, 41-5.
Liu H, Qi B, Guo X, et al (2013). Genetic variations in radiation and chemotherapy drug action pathways and survival in locoregionally advanced nasopharyngeal carcinoma treated with chemoradiotherapy. *PLoS One*, **8**, e82750.
Liu Y, Wang L, Lin XY, et al (2012). Anti-apoptotic effect of claudin-1 on TNF-alpha-induced apoptosis in human breast cancer MCF-7 cells. *Tumour Biol*, **33**, 2307-15.
Locke SM, Martienssen RA (2006). Slicing and spreading of heterochromatic silencing by RNA interference. *Cold Spring Harb Symp Quant Biol*, **71**, 497-503.
Lu TY, Kao CF, Lin CT, et al (2009). DNA methylation and histone modification regulate silencing of OPG during tumor progression. *J Cell Biochem*, **108**, 315-25.
Lu Z, Ding L, Lu Q, Chen, YH (2013). Claudins in intestines: Distribution and functional significance in health and diseases. *Tissue Barriers*, **1**, e24978.
Ma AN, Lu J, Zhou XJ, Wang YX (2011). Histone deacetylation directs DNA methylation in survivin gene silencing. *Biochem Biophys Res Commun*, **404**, 268-72.
Marks PA, Richon VM, Miller T, Kelly WK (2004). Histone deacetylase inhibitors. *Adv Cancer Res*, **91**, 137-68.
McBain JA, Eastman A, Nobel CS, Mueller GC (1997). Apoptotic death in adenocarcinoma cell lines induced by butyrate and other histone deacetylase inhibitors. *Biochem Pharmacol*, **53**, 1357-68.
Ou JN, Torrisani J, Unterberger A, et al (2007). Histone deacetylase inhibitor Trichostatin A induces global and gene-specific DNA demethylation in human cancer cell lines. *Biochem Pharmacol*, **73**, 1297-307.
PA Marks RAR, VM Richon RB (2001). Histone deacetylases and cancer: causes and therapies. *Nature Reviews Cancer*, **1**, 194-202.
Platta CS, Greenblatt DY, Kunnimalaiyaan M, Chen H (2007). The HDAC inhibitor trichostatin A inhibits growth of small cell lung cancer cells. *J Surg Res*, **142**, 219-26.
Qin, L, Zhang, X, Zhang, L, et al (2008). Downregulation of BMI-1 enhances 5-fluorouracil-induced apoptosis in nasopharyngeal carcinoma cells. *Biochem Biophys Res Commun*, **371**, 531-5.
Roth SY, Denu JM, Allis CD (2001). Histone acetyltransferases. *Annu Rev Biochem*, **70**, 81-120.
Saha RN, Pahan K (2006). HATs and HDACs in neurodegeneration: a tale of disconcerted acetylation homeostasis. *Cell Death Differ*, **13**, 539-50.
Selker EU (1998). Trichostatin A causes selective loss of DNA methylation in Neurospora. *Proc Natl Acad Sci USA*, **95**, 9430-5.
Shin JY, Kim HS, Lee KS, et al (2000). Mutation and expression of the p27KIP1 and p57KIP2 genes in human gastric cancer. *Exp Mol Med*, **32**, 79-83.
Shiva STV, Willems L (2014). Epigenetic modulators mitigate angiogenesis through a complex transcriptomic network. *Vascul Pharmacol*, **???**.
Siddik ZH (2003). Cisplatin: mode of cytotoxic action and molecular basis of resistance. *Oncogene*, **22**, 7265-79.
Sigalotti L, Fratta E, Coral S, Maio M (2013). Epigenetic drugs as immunomodulators for combination therapies in solid tumors. *Pharmacol Ther*, 142, 339-50.
Smith BC, Denu JM (2009). Chemical mechanisms of histone lysine and arginine modifications. *Biochim Biophys Acta*, **1789**, 45-57.
Spano JP, Busson P, Atlan D, et al (2003). Nasopharyngeal carcinomas: an update. *Eur J Cancer*, **39**, 2121-35.
Thiagalingam S, Cheng KH, Lee HJ, et al (2003). Histone deacetylases: unique players in shaping the epigenetic histone code. *Ann N Y Acad Sci*, **983**, 84-100.
Tian F, Yip SP, Kwong DL, et al (2013). Promoter hypermethylation of tumor suppressor genes in serum as potential biomarker for the diagnosis of nasopharyngeal carcinoma. *Cancer Epidemiol*, **37**, 708-13.
Tse C, Sera T, Wolffe AP, Hansen JC (1998). Disruption of higher-order folding by core histone acetylation dramatically enhances transcription of nucleosomal arrays by RNA polymerase III. *Mol Cell Biol*, **18**, 4629-38.
Tsuji N, Kobayashi M, Nagashima K, et al (1976). A new antifungal antibiotic, trichostatin. *J Antibiot*, **29**, 1-6.
Vaillant I, Paszkowski J (2007). Role of histone and DNA methylation in gene regulation. *Curr Opin Plant Biol*, **10**, 528-33.
Villar-Garea A, Esteller M (2004). Histone deacetylase inhibitors: understanding a new wave of anticancer agents. *Int J Cancer*, **112**, 171-8.
Wang JJ, Liu Y, Zheng Y, et al (2012). Comparative proteomics analysis of colorectal cancer. *Asian Pac J Cancer Prev*, **13**, 1663-6.
Wang X, He C, Moore SC, Ausio J (2001). Effects of histone acetylation on the solubility and folding of the chromatin fiber. *J Biol Chem*, **276**, 12764-8.
Wee JT, Ha TC, Loong SL, Qian CN (2010). Is nasopharyngeal cancer really a "Cantonese cancer". *Chin J Cancer*, **29**,

517-26.
Wozniak RJ, Klimecki WT, Lau SS, et al (2007). 5-Aza-2'-deoxycytidine-mediated reductions in G9A histone methyltransferase and histone H3 K9 di-methylation levels are linked to tumor suppressor gene reactivation. *Oncogene*, **26**, 77-90.
Zhang B, Qu JQ, Xiao L, et al (2012). Identification of heat shock protein 27 as a radioresistance-related protein in nasopharyngeal carcinoma cells. *J Cancer Res Clin Oncol*, **138**, 2117-25.
Zhang GQHFYLF (2008). Effects of trichostatin A (TSA) on growth and gene expression in HeLa cells. *Chin Germ J Clin Oncol*, 304-8.
Zhang QC, Jiang SJ, Zhang S, Ma XB (2012). Histone deacetylase inhibitor trichostatin A enhances anti-tumor effects of docetaxel or erlotinib in A549 cell line. *Asian Pac J Cancer Prev*, **13**, 3471-6.